ACS OMEGA

http://pubs.acs.org/journal/acsodf

Article

Polystyrene Macroporous Magnetic Nanocomposites Synthesized through Deep Eutectic Solvent-in-Oil High Internal Phase Emulsions and Fe_3O_4 Nanoparticles for Oil Sorption

Carolina L. Recio-Colmenares, Daniela Ortíz-Rios, José B. Pelayo-Vázquez, Edgar D. Moreno-Medrano, Jenny Arratia-Quijada, José R. Torres-Lubian, Silvia T. Huerta-Marcial, Josué D. Mota-Morales, and María G. Pérez-García*

Cite This: *ACS Omega* 2022, 7, 21763−21774

Read Online

ACCESS | Metrics & More | Article Recommendations | Supporting Information

ABSTRACT: In this work, we report a nonaqueous one-step method to synthesize polystyrene macroporous magnetic nanocomposites through high internal phase emulsions (HIPEs) formulated with the deep eutectic solvent (DES) composed of urea:choline chloride (U:ChCl, in a 2:1 molar ratio) as the internal phase and co-stabilized with mixtures of Span 60 surfactant and non-functionalized magnetite nanoparticles (Fe_3O_4 NPs). The porous structure and the magnetic and lipophilic properties of the nanocomposite materials were easily tailored by varying the amount of Fe_3O_4 NPs (0, 2, 5 and 10 wt %) and the surfactant Span 60 (0, 5, 10, and 20 wt %) used in the precursor emulsion. The resultant nanocomposite polyHIPEs exhibit high sorption capacity toward different oils (hexane, gasoline, and vegetable oil) due to their high porosity, interconnectivity, and hydrophobic surface. It was observed that the oil sorption capacity was improved when the amount of surfactant decreased and Fe_3O_4 NPs increased in HIPE formulation. Therefore, polyHIPE formulated with 5 and 10 wt % Span 60 and Fe_3O_4 NPs, respectively, showed the highest oil sorption capacities of 4.151, 3.556, and 3.266 g g^{-1} for gasoline, hexane, and vegetable oil, respectively. In addition, the magnetic monoliths were reused for more than ten sorption/desorption cycles without losing their oil sorption capacity.

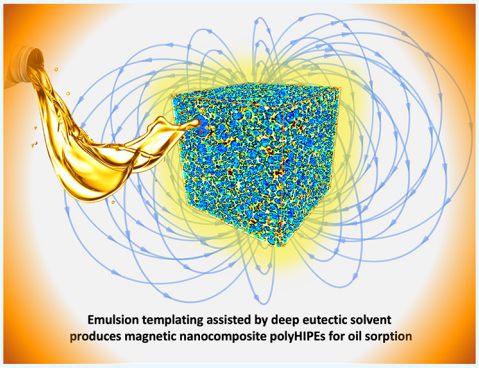

INTRODUCTION

Currently, oil spills are of great concern because they cause serious damage to the environment and threaten human health.[1,2] Several methods have been reported to remove the spilled oils from the ocean, including in situ combustion,[3] chemical treatment,[4] bioremediation with microorganisms or biological agents,[5,6] and mechanical treatment with oil−water gelators or sorbents.[7] Mechanical treatment using sorbents has been recognized as a preferable method over others since it can remove and recover the spilled oils with efficiency, ease, and low cost.[8−10] Therefore, the development and application of oil sorbents have received considerable attention and represented a current challenging task.

A wide variety of oil sorbents have been investigated, such as inorganic materials (e.g., zeolites, silica, clays, etc.),[11−13] natural materials (e.g., cotton, floss, wool, etc.),[14,15] carbon nanotubes,[16−18] graphene,[19,20] and porous polymers,[21−24] among others. Among these materials, porous polymers obtained through high internal phase emulsions (HIPEs) have demonstrated high oil removal capacity and fast oil sorption rates because they commonly possess an interconnected macroporous structure and high pore volume; additionally, their porous surface can be modified for target sorbates.[23−26]

HIPEs are characterized by an internal phase volume exceeding 74% that is dispersed within a polymerizable continuous phase. The structure of HIPEs consists of polyhedral and polydisperse droplets separated by a thin film of the continuous phase that can be polymerized to yield 3D macroporous materials commonly known as polyHIPEs.[27,28] The porous structure of these materials can be easily tailored by modifying the concentration and type of surfactant, the internal to continuous phase volume ratio, the cross-linked concentration used in HIPE formulation,[29,30] and the initiation locus of HIPE polymerization.[31−33] In addition to surfactants, emulsions can be also stabilized with different types of particles (ranging from micrometers to nanometers), which are known

Received: March 26, 2022
Accepted: June 2, 2022
Published: June 13, 2022

as Pickering HIPEs.[34−38] The incorporation of particles can increase emulsion stability due to particles' tendency to adsorb quasi-irreversibly to the oil−water interface, which avoids the phenomena of coalescence and Ostwald ripening.[39−43] After HIPE polymerization, particles remain embedded onto the porous surface of the resultant (nano)composite polyHIPE. Thus, the use of particles in HIPE formulation not only can replace or reduce the amount of surfactant but also is an accessible method for surface porous functionalization.[39,40] It has been reported that nanocomposite materials with different properties (e.g., mechanical,[26,41,42] thermal,[43] electrical,[44] magnetic,[38,45] lipophilic[38,45]) can be obtained by the inclusion of nanoparticles. For instance, nanoparticles (NPs) of silicon carbide,[46] magnetite (Fe_3O_4),[47,48] carbon nanotubes,[26] and cellulose[49] have allowed improvement of lipophilic properties that enhance the oil absorption performance of different nanocomposite polyHIPEs.

Some works[50−54] have reported the inclusion of functionalized Fe_3O_4 nanoparticles to obtain magnetic nanocomposite polyHIPEs *via* Pickering emulsions. For example, Zhou *et al.*[50] functionalized Fe_3O_4 nanoparticles by either carboxylic acid (RCOOH) or silane coupling agents ($RSi(OC_2H_5)_3$) to increase their hydrophobicity in order to obtain stable Pickering emulsions with polar oils. The droplet size and conductivity of the W/O emulsions were weakly influenced by the coating type, coating extent, and modifier alkyl chain length. In addition, the average droplet size and the volume fraction of stable emulsions increased with the increase in the oil/water ratio. In another research, Fe_3O_4-cellulose nanocrystals were used to stabilize O/W Pickering emulsions.[51] Both pH and magnetite responses were investigated. Stable emulsions were obtained at pH 3−6, and the magnetic test showed that the emulsion droplet diameter influences the magnetic response, and the motion of smaller droplets diameter toward the magnet was much faster as compared to the bigger ones.[51] It should be noted that in these studies, unmodified Fe_3O_4 NPs are unable to stabilize W/O Pickering emulsions.[50,51] Other works[34,55,56] also reported that the functionalization of nanoparticles can offer better results in the stability of emulsions; however, there is a latent need to obtain nanocomposite macroporous materials with bare nanoparticles exposed onto their porous surface for different applications including water treatment,[26,45] tissue engineering,[41,42] support for chemical reactions,[57] and electricity generation.[44] Therefore, there is a great interest to develop new techniques that allow the integration of non-functionalized NPs *via* Pickering emulsion to obtain nanocomposite polyHIPEs.

Recently, deep eutectic solvents (DESs) have emerged as non-aqueous alternatives to the internal or continuous phase of HIPEs.[25,26,30,41,42,58,59] DESs are a new generation of green solvents described as eutectic mixtures of ammonium salts (acting as hydrogen-bond acceptors, HBAs) and non-ionic hydrogen-bond donors (HBDs).[60] HBA and HBD components are capable of self-association, often through hydrogen bonding interactions, to form eutectic systems with a melting point lower than the individual components. In addition, DESs are considered designer solvents because their properties (e.g., viscosity, solubility, biocompatibility, biodegradability, thermal property, etc.) can be easily modified by choosing both the nature and the ratio of their components.[60] The formulation of HIPEs using DES as the internal phase was first reported by Carranza et al.[61] These researchers formulated HIPEs using a DES composed of urea (U) and choline chloride (ChCl) in a 2:1 molar ratio as the internal phase and different methacrylates as the continuous phase. HIPEs were polymerized at low pressure due to the negligible volatility of the DES, thus significantly expanding on the polymerization conditions available for poly(HIPE) synthesis.[61] Subsequently, styrenic polyHIPEs were synthesized through the formulation of emulsions with DES of different viscosities.[30] U, glycerol (Gly), and ethylene glycol (EGly) were used as HBDs and ChCl as HBA. It was observed that DES viscosity was essential to enhance HIPE stability. A decrease in pore size and an increase in the degree of openness were achieved when the U:ChCl DES (DES with the highest viscosity of 750 cP at 25 °C) was used as the internal phase in HIPE formulation. It is important to point out that an open macroporous structure is one of the main aspects in the synthesis of polyHIPEs and it is commonly controlled through the incorporation of large quantities of surfactant, which is later removed. The high amount of surfactant can lead to an environmental impact and cost rise. Furthermore, the mechanical and morphological properties of the macroporous materials can be affected.[30] The use of DES allowed the synthesis of polyHIPEs with controlled pore size decreasing the amount of surfactant compared with that required in aqueous HIPE formulation.[30,58] On the other hand, it has been reported that DESs' intrinsic properties facilitate the release of non-functionalized nanomaterials toward the interface of Pickering HIPEs from a bottom-up approach that allows the selective introduction of interfacial functionality into polyHIPEs.[26,41,42] For instance, HIPEs formulated with U:ChCl DES were stabilized with nitrogen-doped multiwalled carbon nanotubes (MWTCNTs) and surfactant mixtures.[26] These emulsions served as templates to obtain poly(styrene) and poly(methyl methacrylate) nanocomposite polyHIPEs. MWTCNTs were deposited onto the porous surface, which increased the hydrophobicity and pore openness of the obtained polyHIPEs for the selectivity sorption of fuels. All these results revealed that DESs have emerged as a promising green tool for the creation of macroporous nanocomposites with controlled surface properties.

In this work, the U:ChCl DES was used as the internal phase of styrene-based HIPEs co-stabilized with the surfactant Span 60 and non-functionalized Fe_3O_4 NPs. Additionally, HIPEs formulated with water were comparatively studied. The high viscosity of the U:ChCl DES (750 cP at 25 °C[62,63]) played an important role in obtaining stable emulsions and facilitated the release of Fe_3O_4 NPs toward the DES/oil interface. After emulsion polymerization, nanocomposite polyHIPEs with well-defined interconnected macroporous structures and Fe_3O_4 NPs deposited onto their porous surface were exclusively obtained when the U:ChCl DES was used as the internal phase. Furthermore, co-stabilization of DES-in-oil HIPEs was investigated by varying the concentrations of Fe_3O_4 NPs (0, 2, 5, and 10 wt % with respect to the continuous phase) and the surfactant Span 60 (0, 5, 10 and 20 wt % with respect to the continuous phase). The synergistic association between Fe_3O_4 NPs and Span 60 was essential to enhance the stability of DES-in-oil HIPEs and allowed the modification of the porous structure and the magnetic and lipophilic properties of the resultant nanocomposite polyHIPEs. These materials were successfully applied as selective sorbents for different oils (such as gasoline, hexane, and vegetable oil), showing a competitive performance and reusability.

https://doi.org/10.1021/acsomega.2c01836
ACS Omega 2022, 7, 21763−21774

MATERIALS AND METHODS

Materials. Styrene (St, ≥99%), divinylbenzene (DVB, ≥99%), choline chloride (ChCl, ≥98%), urea (U, ≥99%), Span 60 (sorbitan monostearate), magnetite nanoparticles (Fe_3O_4 NPs, 97%, average particle size 50−100 nm), potassium persulfate (KPS, 99%), and hexane were purchased from Sigma-Aldrich. Vegetable oil, gasoline (Magna 87 octane), and ethanol were obtained from Golden Bell. Doubly distilled and deionized water was employed. All materials were used without further purification.

Preparation and Characterization of HIPEs. The internal nonaqueous DES phase with a high viscosity of 750 cP was prepared according to other works reported.[62,63] ChCl was combined with U in a 1:2 molar ratio. The mixture was heated at 60 °C until a clear viscous and homogeneous liquid was obtained. ChCl was oven-dried at 90 °C before use to remove all moisture. Subsequently, DES-in-oil and W/O HIPEs were prepared by dropwise addition of the internal phase (DES or water, 80 vol %) to the continuous phase formed by St:DVB in a 10:1 molar ratio, respectively, in a 5 mL glass vial while vortexing at 3200 rpm for 10 min at 25 °C. The formulated emulsions were stabilized using different amounts of Span 60 (0, 5, 10, and 20 wt %) and magnetite nanoparticles (0, 2, 5, and 10 wt %) with respect to the continuous phase. Emulsions were named HIPE-*X*S-*Y*NP-Z, where *X* is the amount of surfactant, *Y* is the amount of Fe_3O_4 NPs, and Z is the type of dispersed phase (W for water and U for the U:ChCl DES). HIPE morphology was studied by optical microscopy (Olympus BX51) with a camera QICAM (FAST1394) and the software Linksys 32. The droplet size was determined in sets of 100 using Image J analysis software.

Synthesis and Characterization of Magnetic Nanocomposite polyHIPEs. To synthesize the macroporous magnetic nanocomposites (polyHIPEs), the continuous phase consisting of St-DVB was polymerized by free radicals using KPS as the initiator (10 wt % with respect to the monomers) added to the internal phase. Polymerization was carried out at 60 °C for 24 h. After polymerization, monoliths were washed by shaking (orbital shaker at 150 rpm) with water for 3 days and then with ethanol for 1 day to remove the dispersed phase and then dried in an oven at 37 °C for 24 h. PolyHIPEs were named prefixing P to their precursor HIPE. Conversion was determined gravimetrically by dividing the mass of the dried monolith by its expected mass.

The total pore volume was determined using the equation $V_T = \frac{1}{\rho_b} - \frac{1}{\rho_w}$, according to other works reported.[25,30,41,44] ρ_b is the polyHIPE bulk density calculated by measuring the volume of monoliths with regular shape, and ρ_w is the wall density that corresponded to the polymer density (1.05 g cm^{-3}).[30] The polyHIPE macroporous morphology was observed by field-emission scanning electron microscopy (FESEM, Mira from TESCAN) at an accelerating voltage of 15 kV and a working distance of 14 mm. All samples were gold-coated. The size of the pores and the windows between the pores were calculated in sets of 100 image readings using ImageJ analysis software. These values were used to estimate the degree of openness of the macroporous monoliths according to the Pulko and Krajnc equation,[64] $O = \frac{N \times d^2}{4 \times D^2}$, where *O* is polyHIPE openness, *N* is the average number of visible pore windows, *d* is the average pore window diameter, and *D* is the average pore diameter.

To determine the presence of magnetite NPs onto the porous structure of the polyHIPEs, elemental mapping was carried out using energy dispersive X-ray spectroscopy (EDS, Bruker). In addition, magnetic monoliths were analyzed by X-ray diffraction (XRD, Empyrean diffractometer) with Cu Kα radiation from 5 to 90° (0.02° step size and 30 s counting time). Thermogravimetric analysis (TGA) was performed on a TA Q500 V 6.7 instrument. The magnetic monoliths were heated to 600 °C in N_2 at a scan rate of 10 °C min^{-1}, and the observed mass loss was attributed to quantitative pyrolysis of the polymeric component. The magnetization curves were measured at room temperature under varying magnetic field from −9000 to +9000 Oe on a 9500 microprocessor-controlled vibrating sample magnetometer (VSM). Furthermore, polyHIPEs were analyzed to determine their hydrophobic properties using a contact angle measuring system (OCA, DataPhysics with SCA20 software).

For the sorption−desorption test, the sorption capacity (*Q*) of the monoliths for vegetable oil, gasoline, hexane, and water was investigated by using a batch technique at room temperature. A magnetic polyHIPE (25 mg) was added to 50 mL of oil or water at different times. *Q* was determined by the equation $Q = (W - W_0)/W_0$, where W_0 and *W* are the weights of the magnetic monolith before and after sorption at different times, respectively. *Q* is expressed in terms of mass of oil or water absorbed per gram of dry monolith. After the sorption process, the monoliths were centrifuged at 4000 rpm to obtain the absorbed oil or water and determine the number of sorption/desorption cycles of the monoliths.

RESULTS AND DISCUSSION

Synthesis and Characterization of Magnetic Styrene-Based HIPEs Formulated with Either DES (U:ChCl) or Water as the Internal Phase. Nanoparticles (NPs) can be used effectively as emulsifying agents to obtain emulsions with controlled droplet sizes when their specific surface-functionalization allows for kinetic adsorption that in turn supports the formation of an effective diffusion barrier layer at the interface.[65,66] However, when the barrier cannot be formed solely by NPs, the incorporation of molecular surfactants can increase the stability of the emulsion through a co-stabilization effect between the NPs and the surfactant.[65,66] Herein, HIPEs were formulated with a continuous phase (20 vol %) composed of styrene and divinylbenzene (10:1 molar ratio, respectively), Span 60, and non-functionalized Fe_3O_4 NPs (50−100 nm diameter). Span 60 was employed due to its low hydrophilic/hydrophobic balance value (HLB) of 4.7, which is suitable for stabilizing water-in-oil (W/O) and DES-in-oil emulsions.[30] Fe_3O_4 NPs were added to provide magnetic properties to the materials, but its co-stabilizing effect with Span 60 was also evaluated. Accordingly, different amounts of Span 60 (0, 5, 10, and 20 wt %) and Fe_3O_4 NPs (0, 2, 5, and 10 wt %) were used with respect to the continuous phase. The U:ChCl DES (2:1 molar ratio) was selected as the dispersed phase (80 vol %) due to its polarity and high viscosity (750 cP at 25 °C[62,63]), characteristics that have been demonstrated to be central for stable nonaqueous HIPE formation. Pérez-García *et al.*[30] demonstrated that DESs with high viscosities used as the dispersed phase in the formulation of styrene-based HIPEs increase the stability of the emulsions. In the same line, Huerta-Marcial and Mota-Morales demonstrated that not only the DESs' viscosity but also the homogenization method vortexing or high-speed homogenizer affects the stability and

https://doi.org/10.1021/acsomega.2c01836
ACS Omega 2022, 7, 21763−21774

Table 1. Stability and Structural Morphology of HIPEs and polyHIPEs, Magnetite Nanoparticle Content (%Fe_3O_4 NPs) Calculated from Thermogravimetric Analysis (TGA), Conversion Based on Gravimetry, and Magnetic Saturation of polyHIPEs[b]

	HIPE		polyHIPE						
code	stability (h)	droplet diameter (μm)	pore diameter (μm)	pore window (μm)	O (%)	X (%)	% Fe_3O_4 NPs (wt %)[a]	magnetic saturation (emu g^{-1})	V_T (cm^3g^{-1})
5S-5NP-U	12	6.5 ± 0.54	7.3 ± 1.01	1.50	12.0	92	5.4	7.8	3.7
5S-10NP-U	14	6.1 ± 0.35	6.1 ± 0.12	1.40	8.5	93	11.7	12.1	4.3
10S-0NP-U	14	6.1 ± 0.14	5.4 ± 0.71	1.30	13.0	95	0	0	4.4
10S-2NP-U	16	4.7 ± 0.14	5.2 ± 0.71	1.20	13.0	95	2.4	3.1	4.4
10S-5NP-U	>16	4.6 ± 0.02	5.1 ± 0.86	1.13	12.6	95	5.7	7.9	4.5
10S-10NP-U	>16	4.5 ± 0.04	5.0 ± 0.97	1.12	9.7	95	12.1	12.9	4.8
20S-0NP-U	>16	4.8 ± 0.20	4.9 ± 0.14	1.29	13.5	96	0	0	4.8
20S-2NP-U	>16	4.2 ± 0.09	4.3 ± 0.01	1.17	13.2	95	2.9	2.8	4.8
20S-5NP-U	>16	4.1 ± 0.48	4.1 ± 0.15	1.10	12.9	95	5.9	8.0	4.9
20S-10NP-U	>16	3.4 ± 0.09	3.5 ± 1.01	0.90	10.1	95	12.5	13.5	5.1

[a]Measured by TGA. Weight percent with respect to the total amount of polymer. [b]V_T: total pore volume. X: conversion, O: degree of openness.

droplet size of HIPEs.[59] Therefore, to comparatively evaluate the stabilizing effect of DES, HIPEs were formulated with water as the dispersed phase, using the same amounts of Span 60 and Fe_3O_4 NPs. The HIPEs were named as HIPE-XS-YNP-Z, where X is the amount of the surfactant, Y is the amount of Fe_3O_4 NPs, and Z is the type of dispersed phase (W for water and U for the U:ChCl DES).

Physical stability of HIPEs was assessed by visual inspection (Table 1). The HIPEs formulated without a surfactant, with both water and DES, and different amounts of Fe_3O_4 NPs (HIPEs-0S-YNP-U and HIPEs-0S-YNP-W, where Y = 0, 2, 5, and 10 wt %) showed phase separation (Figure S1A) within minutes. In the case of the HIPEs formulated with water, HIPEs-5S-YNP-W (Y = 0, 2, 5, and 10 wt %) also showed phase separation and HIPEs-10S-YNP-W and HIPEs-20S-YNP-W (Y = 0, 2, 5, and 10 wt %) underwent phase separation within 1 h. Otherwise, the high viscosity of DES in the HIPEs formulated with the U:ChCl enhanced the stability time (>12 h), which was further extended by increasing the amount of surfactant and Fe_3O_4 NPs (Table 1). HIPEs exhibited a high viscosity and a gel-like appearance (flow resistance upon inversion of their container, Figure S1B). It should be noted that in the case of HIPEs formulated with 5 wt % Span 60 and U:ChCl DES, stable emulsions were exclusively obtained with amounts of Fe_3O_4 NPs equal to or greater than 5 wt %. These results showed that there is a synergism between Fe_3O_4 NPs and Span 60, which plays a crucial role in the stability of HIPEs.

It has been reported that the combination of nanoparticles with surfactants produces a synergistic effect that has been used to improve the stability of emulsions.[66−68] Such synergism leads to improved stability compared with the sole use of a surfactant or particles, becoming a novel approach to form porous materials with open, interconnected structures. Further, provided that nanoparticles remain onto the porous surface after polymerization of the HIPE precursor, this is an advantageous route for the functionalization of the polyHIPE inner surface.[26,41,42] Binks et al.[68] systematically studied the behavior and properties of oil-in-water emulsions stabilized by using dual emulsifiers, finding that the synergy between emulsifiers led to greater emulsion stability. In another study,[67] researchers found that the particles are generally ineffective emulsifiers by their own means. Stable Pickering emulsions are possible only by the particles' functionalization to change their wettability.[51,69] Nevertheless, when used together with surfactants, a co-stabilization effect occurs and, thus, the stability of emulsions is improved.[67] In this context, non-functionalized Fe_3O_4 NPs were incorporated onto the porous surface of monoliths, through a one-step method used for the formulation of the DES-in-oil-HIPEs, where a co-stabilization effect between Fe_3O_4 NPs and the surfactant Span 60 permitted obtaining stable emulsions and the non-functionalized Fe_3O_4 NPs provided magnetic properties to the final polyHIPEs.

The morphology of HIPEs was observed using optical microscopy. Figure 1 shows representative micrographs of the

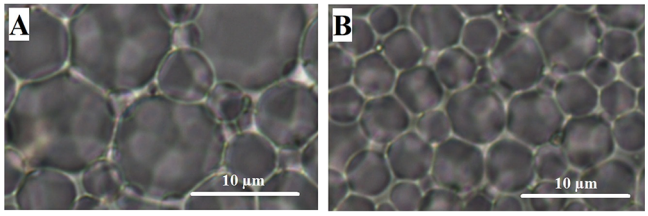

Figure 1. Representative micrographs obtained by optical microscopy of the effect of magnetite NPs on the droplet size of emulsions (A) HIPE-10S-0NP-U and (B) HIPE-10S-10NP-U.

HIPEs without Fe_3O_4 NPs (Figure 1A) and with Fe_3O_4 NPs (Figure 1B). The structure of the HIPEs consists of polyhedral drops separated by a thin film of a continuous phase (St-DVB), which is characteristic of this type of emulsion.[30] Due to the low stability of HIPEs-10S-YNP-W and HIPEs-20S-YNP-W (Y = 0, 2, 5, and 10 wt %), the micrographs could not be obtained (the drops collapsed during observation). From these results, it can be determined that the stability of the emulsions is affected by the type of dispersed phase. Herein, the HIPEs formulated with the U:ChCl DES presented greater stability compared with those formulated using water.

The high viscosity of the U:ChCl DES drastically reduces the Ostwald ripening effect, thus preventing the collapse of the thin walls of the continuous phase and the collapse of the HIPEs.[30,61] Furthermore, solvatophobic interactions between the counterions of ionic liquids and the hydrocarbon portion of surfactants, as well as cation−anion interactions, have been reported to greatly modify the cloud point of non-ionic surfactants.[70,71] The significant influence on the behavior of

https://doi.org/10.1021/acsomega.2c01836
ACS Omega 2022, 7, 21763−21774

macromolecules (e.g., polymeric surfactants) by ionic liquids can be seen as an extreme case of adding salt to the dispersed phase of W/O emulsions, which drastically stabilizes the emulsions through the decrease of the surfactant cloud point.[72] Taking this into account, Carranza et al.[61] proposed that DESs have a similar effect to the addition of salt into the aqueous internal phase of a HIPE and an analogous effect of ionic liquids; these researchers suggested that DES improves the stability of HIPEs through a decrease in the surfactant cloud point, in addition to a high viscosity provided by specific interaction between the DES's components.

The droplet diameter of HIPEs formulated with U:ChCl DES decreased when the amounts of magnetite NPs and Span 60 were increased (Table 1 and Figure 1). These results demonstrate that the combination of Fe_3O_4 NPs and Span 60 allows the formation of a hybrid, which creates an efficient diffusion barrier at the HIPE interface, hence preventing the coalescence and Ostwald ripening effect between the drops, yielding more stable emulsions with controlled drop sizes.[65,66]

Synthesis and Characterization of Magnetic Nanocomposite polyHIPEs. HIPEs were polymerized by adding potassium persulfate (KPS) to the internal phase (10 wt % with respect to the monomers) at 60 °C for 24 h. Obtained polyHIPEs kept the monolithic shape of the container where the polymerization was carried out (Figure S2). Monolithic polyHIPEs showed conversions equal to or greater than 92% (Table 1).

PolyHIPE monoliths showed an interconnected 3D porous structure with a similar morphology of the precursor emulsion (Figure 2 and Figure S3). It has been reported that the locus of initiation of W/O HIPEs has a significant impact on the morphology of the obtained polyHIPEs.[31−33] When the polymerization was initiated at the interface, using the water-soluble initiator KPS, closed-cell foam with polyhedral-shaped pores was obtained. On the other hand, initiating the polymerization in the continuous phase (monomers), using the oil-soluble initiator azobisisobutyronitrile (AIBN), produced an open-cell foam with spherical pores.[32,33] Accordingly, we have used KPS as the polymerization initiator of DES-in-oil HIPEs. Contrary to the aqueous HIPEs, the use of KPS in the DES internal phase resulted in open-cell, interconnected porous structures, indicating that the interface between the continuous phase and the DES is a determining factor in the formation of open-cell porous architectures regardless of the initiation locus (Figure 2 and Figure S3).

The porous diameter of polyHIPEs prepared with the U:ChCl DES was similar to the droplet diameter of their precursor HIPEs, showing that the emulsions were sufficiently stable during the polymerization process to replicate the emulsion morphology (Table 1). Furthermore, as shown by electron microscopy, magnetite NPs were noticeable onto the porous surface of monoliths (Figure 2B,D,F,H), demonstrating that the one-step method used to synthesize styrene porous magnetic polyHIPEs with an interconnected structure was successful. In the case of polyHIPEs obtained from emulsions formed with water (HIPEs-10S-*Y*NP-W, HIPEs-20S-*Y*NP-W, where Y = 0, 2, 5, and 10 wt %), the structure collapsed during polymerization due to the low stability of the precursor HIPEs (Figure S3). In addition, HIPEs formulated with 30 wt % Span 60 and the different amounts of magnetite NPs (0, 2, 5, and 10 wt %) were also used as a template to obtain magnetic macroporous materials, but monoliths crumbled during the purification process and results were not shown.

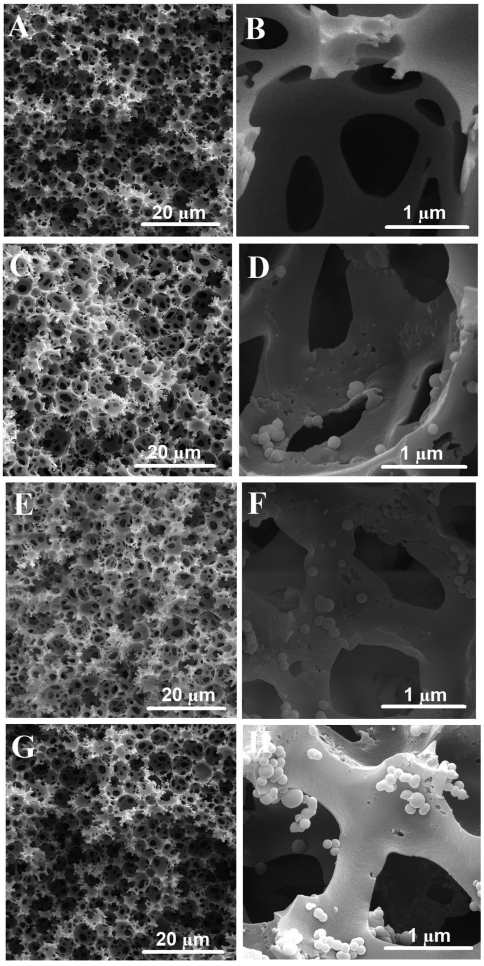

Figure 2. FESEM micrographs of monoliths (A,B) PHIPE-10S-0NP-U, (C,D) PHIPE-10S-2NP-U, (E,F) PHIPE-10S-5NP-U, and (G,H) PHIPE-10S-10NP-U at different magnifications.

Typically, aqueous Pickering-type HIPEs create porous materials with closed structures, regardless of the volume ratio of the continuous and dispersed phase.[65] In HIPEs stabilized solely by surfactants, the surface tension between the oil−water interface is reduced to avoid the coalescence phenomena.[27] As the amount of surfactant increases, the oil layer between the dispersed phase droplets thins during polymerization leading to interconnected windows, meaning a higher degree of openness after polymerization.[30,61] In addition, it has been reported[30,61] that a high increment of surfactant amount can cause the oil layer thinning even more until it disappears, which could explain why it was not possible to obtain monoliths formulated with 30 wt % surfactant. In this case, the amount of surfactant was too high that the monoliths obtained under these conditions had weak walls and the porous structure collapsed. The degree of openness (O) of polyHIPEs obtained was calculated through the relationship between the pore window and the pore diameter values (Table 1), according to Pulko and Krajnc.[64] The results revealed an increase in O when the amount of surfactant increases, at fixed Fe_3O_4 NP content. Therefore, the highest degree of openness was obtained at the highest concentration of surfactant, i.e., 20 wt %. However, an increase in the amount of Fe_3O_4 NPs produces a decrease in O, independent of the amount of surfactant; in this case, the smallest degree of openness

https://doi.org/10.1021/acsomega.2c01836
ACS Omega 2022, 7, 21763−21774

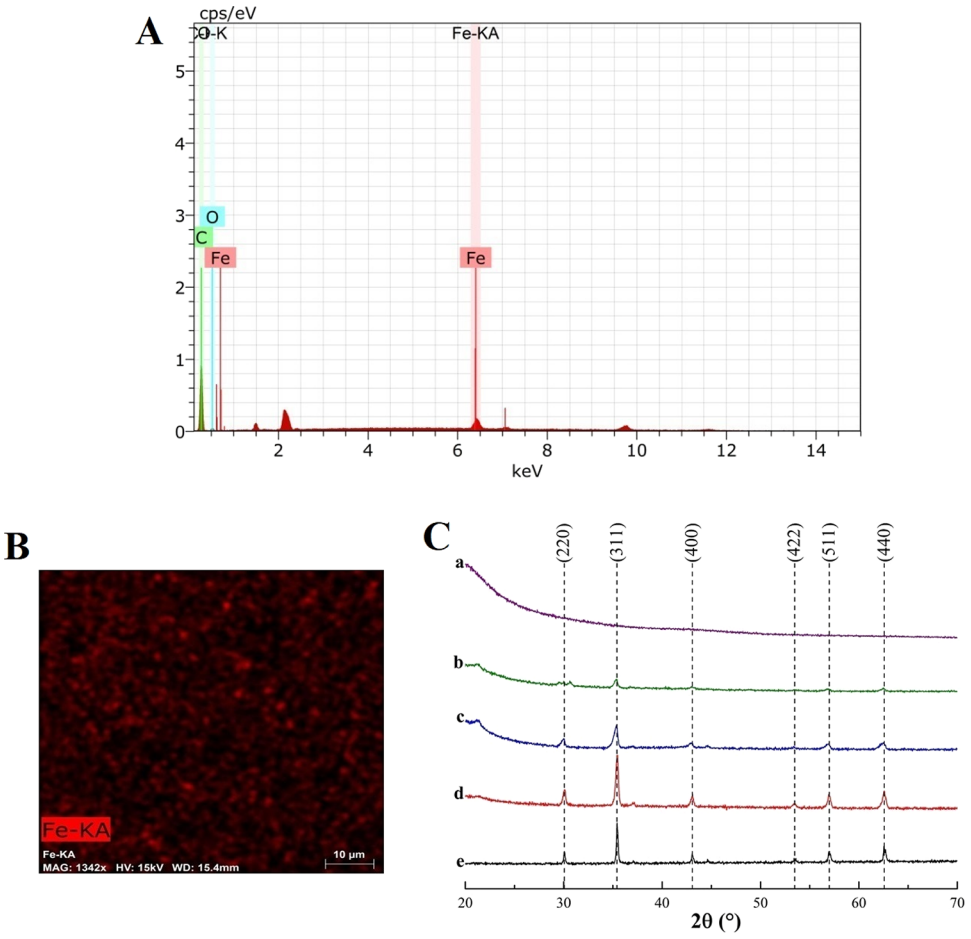

Figure 3. (A) EDS spectra of PHIPE-10S-10NP-U, (B) elemental mapping of PHIPE-10S-10NP-U, and (C) diffractograms of PHIPE- (a) 10S-0NP-U, (b) 10S-2NP-U, (c) 10S-5NP-U, (d) 10S-10NP-U, and (e) pure Fe_3O_4 NPs.

obtained corresponds to 10 wt % NPs. Monoliths presented total pore volume values (V_T) greater than 3.7 $cm^3\ g^{-1}$(Table 1), which are similar to other macroporous materials reported in the literature.[25,30,41]

The presence of Fe_3O_4 NPs, which confers the magnetic property to the monoliths, was determined through energy-dispersive X-ray spectroscopy (EDS). The EDS spectra and the elemental mapping showed the distribution of Fe onto the porous surface of the polystyrene materials (Figure 3A,B). Furthermore, the presence of the magnetite was confirmed by X-ray diffraction. Figure 3C shows representative diffractograms of PHIPE-10S-*Y*NP-U (where *Y* = 2, 5 and 10 wt %). According to Mandal *et al.*,[73] the characteristic diffraction peaks of the Fe_3O_4 crystal represent planes (220), (311), (400), (422), (511), and (440) at diffraction angles of 30.1°, 35.7°, 43.1°, 53.5°, 57.2°, and 62.6°, respectively. The diffractograms showed these characteristic peaks, corresponding to the Fe_3O_4 NPs, hence demonstrating that the polymerization process and the subsequent purification did not modify the crystalline structure of magnetite NPs (Figure 3C and Figure S4). As expected, the diffractograms of the polyHIPEs synthesized without magnetite NPs did not present peaks due to the NP absence.

To determine the thermal stability and the Fe_3O_4 NP content of the monoliths, thermogravimetric analysis (TGA) was carried out (Figure S5). The thermograms revealed a weight loss from 240 to 447 °C for all polyHIPEs. The weight loss can be attributed to the polymer decomposition and the final residue to the amount of magnetite deposited in each material (Table 1), which was similar to the amount of Fe_3O_4 NPs used in the formulation of the emulsions. These results demonstrate that there was no loss of NPs during the washing and drying process of the monoliths. Additionally, the magnetic behavior of the polyHIPEs was measured at 25 °C using a vibrating sample magnetometer (VSM). Magnetization curves revealed that PHIPEs-*X*S-*Y*NP-U (where *X* = 5, 10, and 20 wt % and *Y* = 2, 5, and 10 wt %) were superparamagnetic, which is characteristic of magnetite NPs (Figure S6).[74,75] Moreover, the magnetic saturation increased when increasing the amount of magnetite NPs accordingly (Table 1).

The hydrophobicity of the synthesized materials was determined through the measurement of the contact angle between the monolith solid surface and a droplet of water. The results demonstrated an increment in the contact angle when the amount of NPs incorporated in the material increased (Figure 4). These results are similar to previous works reported.[26,42,76] For example, Zhang *et al.*[76] reported an increase in the contact angle of macroporous poly(styrene) materials by increasing the amount of magnetite nanoparticles, which was attributed to an increase in the roughness of the surface material. Mota-Morales and collaborators observed similar behavior in the contact angle when increasing the amount of nanohydroxyapatite nanoparticles and carbon nanotubes.[26,42] We also noticed an increase in the contact

https://doi.org/10.1021/acsomega.2c01836
ACS Omega 2022, 7, 21763−21774

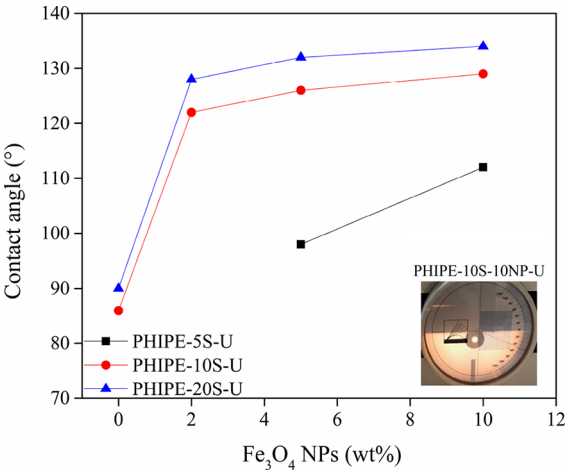

Figure 4. Contact angle of magnetic monoliths synthesized from HIPEs formulated with DES U:ChCl and different amounts of surfactant and magnetite NPs.

angle when increasing the amount of surfactant at a fixed NP concentration. This could be attributed to a smaller pore size, which makes more difficult the diffusion of water within the pores, causing an increase in the contact angle. The synthesized materials presented a hydrophobic surface with contact angles greater than 90°. Furthermore, increasing the amount of nanoparticles and surfactant (up to 10 and 20%, respectively) in the HIPEs precursor resulted in macroporous magnetic nanocomposites with contact angles greater than 120°, a characteristic of superhydrophobic surfaces, therefore increasing their potential use as selective sorbent materials for oils in aqueous media.

Magnetic Porous Polystyrene Nanocomposites with Lipophilic Properties Used as Absorbent Materials for Gasoline, Oil, and Hexane. Research on oil−water separation has received a great deal of attention due to the increasing amount of industrial oily wastewater and frequent oil and hydrocarbon spill accidents.[4−7] Owing to their high pore volume and interconnectivity, sponge-like materials possess ideal characteristics for oil recovery from aqueous

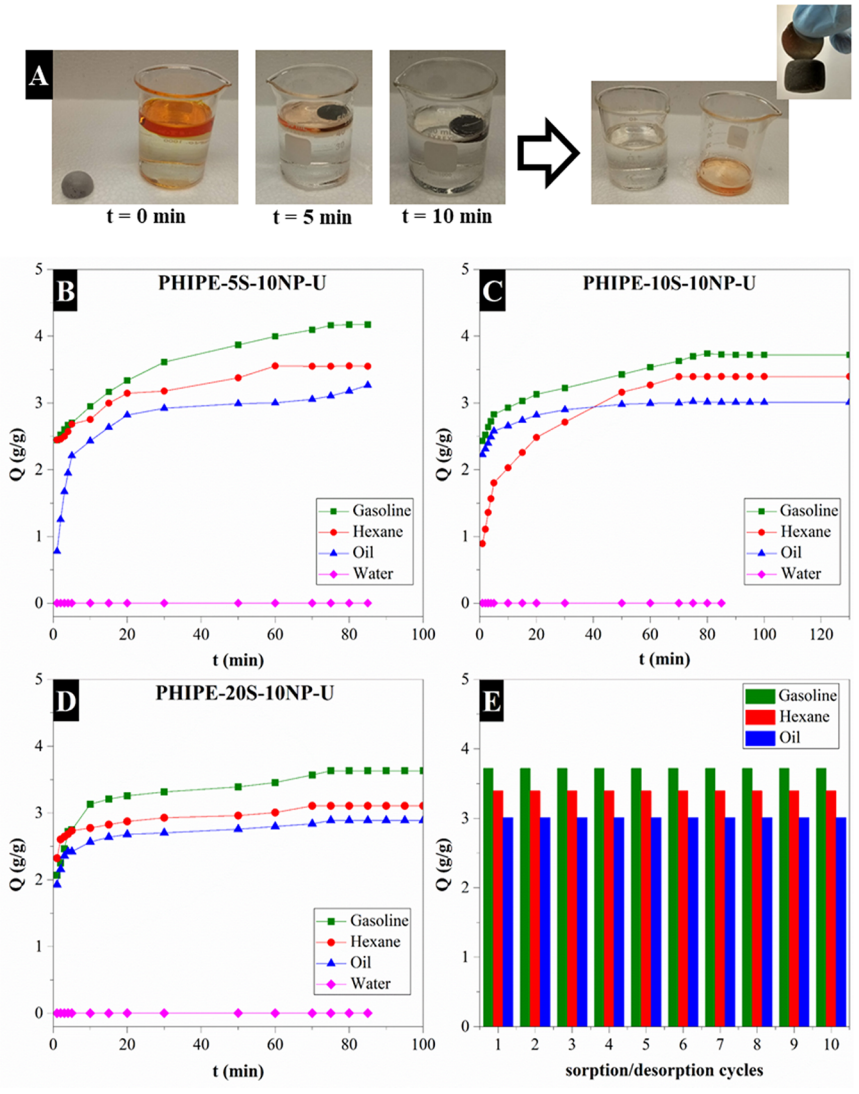

Figure 5. (A) Selectivity of the material in the absorption of gasoline in a water/gasoline mixture, sorption capacity of gasoline, hexane, oil, and water as a function of time for (B) PHIPE-5S-10NP-U, (C) PHIPE-10S-10NP-U, and (D) PHIPE-20S-10NP-U and (E) representative sorption capacity of PHIPE-10S-10NP-U at different sorption/desorption cycles. Sorption conditions: 25 mg of magnetic monolith, 150 mL of oil or hydrocarbon at room temperature.

https://doi.org/10.1021/acsomega.2c01836
ACS Omega 2022, 7, 21763−21774

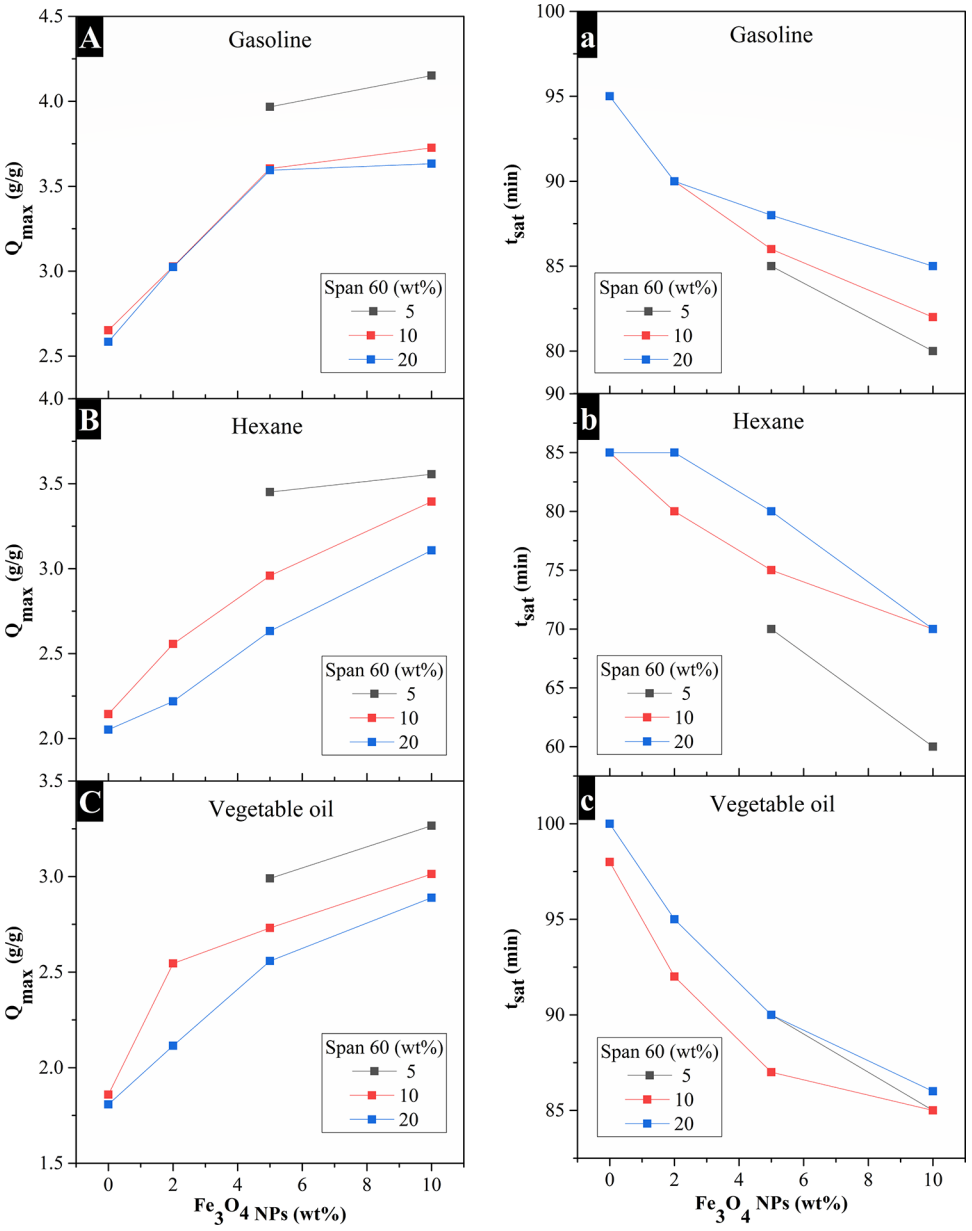

Figure 6. Q_{max} and t_{sat} of (A,a) gasoline, (B,b) hexane, and (C,c) vegetable oil of the monoliths synthesized from HIPEs formulated with DES U:ChCl and different amounts of surfactant and magnetite NPs. Absorption conditions: 25 mg of magnetic monolith, 150 mL of oil or hydrocarbon at room temperature.

media.[21−23] In this work, the nanocomposites polyHIPEs synthesized were used as oil sorbent materials due to their high porosity, interconnectivity, and lipophilic surface, in addition to their easy separation by means of magnetism. For this purpose, sorption experiments were performed by immersing the monoliths in an excess of water, gasoline, hexane, and vegetable oil until reaching the mass in equilibrium to determine the sorption capacity of the materials (Figure 5). As an example, Figure 5A shows the removal of gasoline from a mixture of gasoline and water using the monolith with higher sorption capacity (PHIPE-5S-10NP-U), demonstrating that the obtained materials can be used as selective oil sorbents. Moreover, the monoliths can be manipulated with a magnet due to their magnetic properties and thus are easily removed (Figure 5A).

Figure 5 shows the oil sorption curves as a function of time for PHIPE-5S-10NP-U, PHIPE-10S-10NP-U, and PHIPE-20S-10NP-U. On average, equilibrium is reached in the range of 80−95, 60−85, and 85−100 min for gasoline, hexane, and oil absorption, respectively. On the other hand, water sorption was negligible due to the hydrophobic surface of the monoliths (Figure 5B,C,D). After sorption, the gasoline-saturated monolith was subjected to a centrifugation process (4000 rpm at RT) and gasoline was recovered. The monoliths were reused for more than 10 sorption/desorption cycles without losing their absorption capacity (Figure 5E). Similar results were reported by Carranza *et al.*[26] These researchers synthesized poly(styrene) polyHIPEs functionalized with multiwalled carbon nanotubes (MWTCNTs), which showed a selective sorption of fuels with adsorption capacities ranging from 3.6 to 4.8 times the original material mass and a consistent performance, even after 20 cycles, in monolith recyclability and fuel recovery.

https://doi.org/10.1021/acsomega.2c01836
ACS Omega 2022, 7, 21763−21774

Figure 6 shows the saturation time (t_{sat}) and maximum sorption capacity (Q_{max}). In all cases, the t_{sat} increases slightly with the increase in the amount of surfactant (Figure 6a−c), which could be attributed to smaller pores obtained when a greater amount of surfactant was used in the formulation of the HIPEs (Table 1). A decrease in the pore size restricts the oil diffusion within the material, which might explain the results obtained. Furthermore, the t_{sat} decreases as the amount of NPs increases due to an increase in the contact angle (Figures 4 and 6). The Q_{max} of the materials was analyzed as a function of the concentration of magnetite NPs deposited in each material. The results indicated that there is a greater Q_{max} of polyHIPEs formulated with a lower amount of surfactant (i.e., having larger pores) and with a greater content of nanoparticles (Figure 6A−C). This increase in Q_{max} was attributed to the increase of both the pore size and the contact angle with optimal values of 6.1 μm and 112°, respectively. It is important to note that the monoliths obtained from HIPEs formulated with a lower amount of surfactant presented a higher Q_{max}. The high viscosity of the DES and the synergistic effect of NPs with the surfactant allowed the reduction of the amount of the latter. The obtained maximum sorption capacities of oil and hydrocarbons were similar to those obtained by polyHIPE materials based on PSt-DVB for gasoline (2.55−4.80 g/g), hexane (2.05−3.68 g/g),[26] and poly(L-lactide)/poly(ε-caprolactone) blend for gasoline, heptane, and diesel (2−2.6 g/g)[25] previously reported in the literature.

CONCLUSIONS

We reported a nonaqueous one-step method to synthesize polystyrene porous magnetic polyHIPEs, using DES-in-oil HIPEs as the template. U:ChCl DES was employed as the internal phase of HIPEs, where a co-stabilization effect between Fe_3O_4 NPs and the surfactant Span 60 permitted obtaining stable emulsions. Additionally, emulsions formulated with water, as the dispersed phase, were comparatively studied. The results revealed that U:ChCl DES produces HIPEs with a longer stability time (>12 h) compared with the HIPEs formulated with water (<1 h). The stability of the DES-in-oil HIPEs was further extended by increasing the amounts of surfactant and Fe_3O_4 NPs, showing a synergism between Fe_3O_4 NPs and Span 60. Unexpectedly, the use of KPS as the polymerization initiator in DES-in-oil HIPEs generated open-cell, interconnected porous structures, suggesting that, regardless of the locus of initiation, the use of DES is a determining factor in the formation of open-cell porous architectures. The resulting polyHIPE monoliths showed an interconnected 3D porous structure with a similar morphology to the precursor emulsion. Furthermore, non-functionalized Fe_3O_4 NPs were incorporated onto the porous surface of monoliths, providing them with magnetic and lipophilic properties. The porous magnetic polyHIPEs were used as an oil sorbent of gasoline, hexane, and vegetable oil due to their high porosity, interconnectivity, and hydrophobic surface. It was observed that lower surfactant and higher Fe_3O_4 NPs contents in polyHIPEs give rise to higher contact angles of water and larger pore size, thus providing high oil sorption capacity. Remarkably, PHIPE-5S-10NP-U showed the highest oil sorption capacities of 4.151, 3.556, and 3.266 g g^{-1} for gasoline, hexane, and vegetable oil, respectively. The magnetic monoliths showed a consistent performance, with more than ten sorption/desorption cycles for oil and hydrocarbons, without losing their sorption capacity. Finally, the reduction of the surfactant amount to 5 wt % was possible due to the high viscosity of the U:ChCl DES used as the dispersed phase in the precursor HIPE and the synergistic effect between the surfactant and the Fe_3O_4 NPs in the emulsion stabilization.

ASSOCIATED CONTENT

Supporting Information

The Supporting Information is available free of charge at https://pubs.acs.org/doi/10.1021/acsomega.2c01836.

Photographs of stable HIPEs and magnetic polyHIPEs, FESEM micrographs of PHIPE-5S-5NP-U, PHIPE-5S-10NP-U, PHIPE-10S-0NP-U, PHIPE-10S-2NP-U, PHIPE-10S-5NP-U, PHIPE-10S-10NP-U, and PHIPE-10S-5NP-W, DRX diffractograms, thermogravimetric analysis, and magnetization curves of magnetic polyHIPEs (PDF)

AUTHOR INFORMATION

Corresponding Author

María G. Pérez-García − *Centro Universitario de Tonalá, Universidad de Guadalajara, Tonalá, Jalisco 45425, México;* orcid.org/0000-0002-5030-3662; Email: mariag.perezg@academicos.udg.mx, mgpg100183@gmail.com

Authors

Carolina L. Recio-Colmenares − *Centro Universitario de Tonalá, Universidad de Guadalajara, Tonalá, Jalisco 45425, México;* orcid.org/0000-0001-7103-2710

Daniela Ortíz-Rios − *Centro Universitario de Tonalá, Universidad de Guadalajara, Tonalá, Jalisco 45425, México*

José B. Pelayo-Vázquez − *Centro Universitario de Tonalá, Universidad de Guadalajara, Tonalá, Jalisco 45425, México;* orcid.org/0000-0001-6899-3449

Edgar D. Moreno-Medrano − *Centro Universitario de Tonalá, Universidad de Guadalajara, Tonalá, Jalisco 45425, México*

Jenny Arratia-Quijada − *Centro Universitario de Tonalá, Universidad de Guadalajara, Tonalá, Jalisco 45425, México;* orcid.org/0000-0001-8264-9310

José R. Torres-Lubian − *Centro de Investigación en Química Aplicada, Saltillo, Coahuila 25294, México*

Silvia T. Huerta-Marcial − *Centro de Física Aplicada y Tecnología Avanzada, Universidad Nacional Autónoma de México, Querétaro 76230, México;* orcid.org/0000-0002-3142-2025

Josué D. Mota-Morales − *Centro de Física Aplicada y Tecnología Avanzada, Universidad Nacional Autónoma de México, Querétaro 76230, México;* orcid.org/0000-0001-8257-0709

Complete contact information is available at: https://pubs.acs.org/10.1021/acsomega.2c01836

Author Contributions

The manuscript was written through contributions of all authors. All authors have given approval to the final version of the manuscript.

Funding

This research was supported by the University of Guadalajara through Pro-SNI-UDG 2020−2021 and the Secretary of Public Education (IDCA-25709 511−6/2020−7839).

Notes

The authors declare no competing financial interest.

■ ACKNOWLEDGMENTS

The authors are thankful to Francisco J. Vivanco-Jarero for assistance in the synthesis of PHIPEs-20S-YNP-U (Y = 0, 2, 5, and 10 wt %). C.L.R.-C. and D.O.-R. thank CONACyT for scholarship.

■ REFERENCES

(1) Laffon, B.; Pásaro, E.; Valdiglesias, V. Effects of exposure to oil spills on human health: Updated review. *J. Toxicol. Environ. Health, Part B* **2016**, *19*, 105−128.
(2) Hong, S.; Yoon, S. J.; Kim, T.; Ryu, J.; Kang, S. G.; Khim, J. S. Response to oiled wildlife in the management and evaluation of marine oil spills in South Korea: A review. *Reg. Study Mar. Sci.* **2020**, *40*, No. 101542.
(3) Aurell, J.; Holder, A.; Gullett, B.; Lamie, N.; Arsava, K.; Conmy, R.; Stone, K. Analysis of emissions and residue from methods to improve efficiency of at-sea, in situ oil spill burns. *Mar. Pollut. Bull.* **2021**, *173*, No. 113016.
(4) Pan, Z.; Zhao, L.; Boufadel, M. C.; King, T.; Robinson, B.; Conmy, R.; Lee, K. Impact of mixing time and energy on the dispersion effectiveness and droplets size of oil. *Chemosphere* **2017**, *166*, 246−254.
(5) Alkorta, I.; Garbisu, C. Phytoremediation of organic contaminants in soils. *Bioresour. Technol.* **2001**, *79*, 273−276.
(6) Cheng, J.; Zhu, X.; Ni, J.; Borthwick, A. Palm oil mill effluent treatment using a two-stage microbial fuel cells system integrated with immobilized biological aerated filters. *Bioresour. Technol.* **2010**, *101*, 2729−2734.
(7) Broje, V.; Keller, A. A. Improved Mechanical Oil Spill Recovery Using an Optimized Geometry for the Skimmer Surface. *Environ. Sci. Technol.* **2006**, *40*, 7914−7918.
(8) Madhubashani, A. M. P.; Giannakoudakis, D. A.; Amarasinghe, B. M. W. P. K.; Rajapaksha, A. U.; Kumara, P. T. P.; Triantafyllidis, K. S.; Vithanage, M. Propensity and appraisal of biochar performance in removal of oil spills: A comprehensive review. *Environ. Pollut.* **2021**, *288*, No. 117676.
(9) Chkirida, S.; Zari, N.; Bouhfid, R.; Qaiss, A. Insight into the bionanocomposite applications on wastewater decontamination: Review. *J. Water Process Eng.* **2021**, *43*, No. 102198.
(10) Li, P.; Cai, Q.; Lin, W.; Chen, B.; Zhang, B. Offshore oil spill response practices and emerging challenges. *Mar. Pollut. Bull.* **2016**, *110*, 6−27.
(11) Hammouda, S.; Chen, Z.; An, C.; Lee, K. Recent advances in developing cellulosic sorbent materials for oil spill cleanup: A state-of-the-art review. *J. Cleaner Prod.* **2021**, *311*, No. 127630.
(12) Khaleque, A.; Alam, M. M.; Hoque, M.; Mondal, S.; Haider, J. B.; Xu, B.; Moni, M. A. Zeolite synthesis from low-cost materials and environmental applications: A review. *Environ. Adv.* **2020**, *2*, No. 100019.
(13) Gil, A.; Santamaría, L.; Korili, S. A.; Vicente, M. A.; Barbosa, L. V.; De Souza, S. D.; Ciuffi, K. J. A review of organic-inorganic hybrid clay based adsorbents for contaminants removal: Synthesis, perspectives and applications. *J. Environ. Chem. Eng.* **2021**, *9*, No. 105808.
(14) Deschamps, G.; Caruel, H.; Borredon, M. E. Oil Removal from Water by Sorption on Hydrophobic Cotton Fibers. 2. Study of Sorption Properties in Dynamic Mode. *Environ. Sci. Technol.* **2003**, *37*, 5034−5039.
(15) Radetić, M. M.; Jocić, D. M.; Jovančić, P. M.; Petrović, Z. L.; Thomas, H. F. Recycled Wool-Based Nonwoven Material as an Oil Sorbent. *Environ. Sci. Technol.* **2003**, *37*, 1008−1012.
(16) Gui, X.; Li, H.; Wang, K.; Wei, J.; Jia, Y.; Li, Z.; Fan, L.; Cao, A.; Zhu, H.; Wu, D. Recyclable carbon nanotube sponges for oil absorption. *Acta Mater.* **2011**, *59*, 4798−4804.
(17) Wang, C. F.; Lin, S. J. Robust Superhydrophobic/superoleophilic sponge for effective continuous absorption and expulsion of oil pollutants from Water. *ACS Appl. Mater. Interfaces* **2013**, *5*, 8861−8864.
(18) Gui, X.; Zeng, Z.; Lin, Z.; Gan, Q.; Xiang, R.; Zhu, Y.; Cao, A.; Tang, Z. Magnetic and highly recyclable macroporous carbon nanotubes for spilled oil sorption and separation. *ACS Appl. Mater. Interfaces* **2013**, *5*, 5845−5850.
(19) Cho, E.-C.; Hsiao, Y.-S.; Lee, K.-C.; Huang, J.-H. Few-layer graphene based sponge as a highly efficient, recyclable and selective sorbent for organic solvents and oils. *RSC Adv.* **2015**, *5*, 53741−53748.
(20) Wang, J.; Zhang, Y.; Liu, Y.; Zheng, W.; Lee, L. P.; Sun, H. B. Recent developments in superhydrophobic graphene and graphene-related materials: from preparation to potential applications. *Nanoscale* **2015**, *7*, 7101−7114.
(21) Tan, D.; Fan, W.; Xiong, W.; Sun, H.; Li, A.; Deng, W.; Meng, C. Study on adsorption performance of conjugated microporous polymers for hydrogen and organic solvents: The role of pore volume. *Eur. Polym. J.* **2012**, *48*, 705−711.
(22) Xue, Z.; Sun, Z.; Cao, Y.; Chen, Y.; Tao, L.; Li, K.; Wei, Y. Superoleophilic and superhydrophobic biodegradable material with porous structures for oil absorption and oil−water separation. *RSC Adv.* **2013**, *3*, 23432−23437.
(23) Zhang, N.; Zhong, S.; Chen, T.; Zhou, Y.; Jiang, W. Emulsion-derived hierarchically porous polystyrene solid foam for oil removal from aqueous environment. *RSC Adv.* **2017**, *7*, 22946−22953.
(24) Cui, X.; Shao, H.; Song, Y.; Yang, S.; Wang, F.; Liu, H. Preparation of highly interconnected porous polymer microbeads *via* suspension polymerization of high internal phase emulsions for fast removal of oil spillage from aqueous environments. *RSC Adv.* **2019**, *9*, 25730−25738.
(25) Pérez-García, M. G.; Gutiérrez, M. C.; Mota-Morales, J. D.; Luna-Bárcenas, G.; Del Monte, F. Synthesis of Biodegradable Macroporous Poly(l -lactide)/Poly(ϵ-caprolactone) Blend Using Oil-in-Eutectic-Mixture High-Internal-Phase Emulsions as Template. *ACS Appl. Mater. Interfaces* **2016**, *8*, 16939−16949.
(26) Carranza, A.; Pérez-García, M. G.; Song, K.; Jeha, G. M.; Diao, Z.; Jin, R.; Bogdanchikova, N.; Mota-Morales, J. D. Deep-Eutectic Solvents as MWCNT Delivery Vehicles in the Synthesis of Functional Poly(HIPE) Nanocomposites for Applications as Selective Sorbents. *ACS Appl. Mater. Interfaces* **2016**, *8*, 31295−31303.
(27) Silverstein, M. S. PolyHIPEs: Recent advances in emulsion-templated porous polymers. *Prog. Polym. Sci.* **2014**, *39*, 199−234.
(28) Zhang, T.; Sanguramath, R. A.; Israel, S.; Silverstein, M. S. Emulsion Templating: Porous Polymers and Beyond. *Macromolecules* **2019**, *52*, 5445−5479.
(29) Lissant, K. The geometry of high-internal-phase-ratio emulsions. *J. Colloid Interface Sci.* **1966**, *22*, 462−468.
(30) Pérez-García, M. G.; Carranza, A.; Puig, J. E.; Pojman, J. A.; del Monte, F.; Luna-Barcenas, G.; Mota-Morales, J. D. Porous monoliths synthesized via polymerization of styrene and divinyl benzene in nonaqueous deep-eutectic solvent-based HIPEs. *RSC Adv.* **2015**, *5*, 23255−23260.
(31) Gurevitch, I.; Silverstein, M. S. Nanoparticle-Based and Organic-Phase-Based AGET ATRP PolyHIPE Synthesis within Pickering HIPEs and Surfactant-Stabilized HIPEs. *Macromolecules* **2011**, *44*, 3398−3409.
(32) Quell, A.; De Bergolis, B.; Drenckhan, W.; Stubenrauch, C. How the Locus of Initiation Influences the Morphology and the Pore Connectivity of a Monodisperse Polymer Foam. *Macromolecules* **2016**, *49*, 5059−5067.
(33) Robinson, J. L.; Moglia, R. S.; Stuebben, M. C.; McEnery, M. A.; Cosgriff-Hernandez, E. Achieving Interconnected Pore Architecture in Injectable PolyHIPEs for Bone. *Tissue Eng., Part A* **2014**, *20*, 1103−1112.
(34) Ikem, V. O.; Menner, A.; Bismarck, A. High-Porosity Macroporous Polymers Sythesized from Titania-Particle-Stabilized

https://doi.org/10.1021/acsomega.2c01836
ACS Omega 2022, 7, 21763−21774

Medium and High Internal Phase Emulsions. *Langmuir* **2010**, *26*, 8836−8841.
(35) Leal-Calderon, F.; Schmitt, V. Solid-stabilized emulsions. *Curr. Opin. Colloid Interface Sci.* **2008**, *13*, 217−227.
(36) Arditty, S.; Whitby, C. P.; Binks, B. P.; Schmitt, V.; Leal-Calderon, F. Some general features of limited coalescence in solid-stabilized emulsions. *Eur. Phys. J. E: Soft Matter Biol. Phys.* **2003**, *11*, 273−281.
(37) Binks, B. P. Particles as surfactants - Similarities and differences. *Curr. Opin. Colloid Interface Sci.* **2002**, *7*, 21−41.
(38) Silverstein, M. S. Emulsion-templated porous polymers: A retrospective perspective. *Polymer* **2014**, *55*, 304−320.
(39) Zafeiri, I.; Horridge, C.; Tripodi, E.; Spyropoulos, F. Emulsions Co-Stabilised by Edible Pickering Particles and Surfactants: The Effect of HLB Value. *Colloid Interface Sci. Commun.* **2017**, *17*, 5−9.
(40) Chevalier, Y.; Bolzinger, M. A. Emulsions stabilized with solid nanoparticles: Pickering emulsions. *Colloids Surf., A* **2013**, *439*, 23−34.
(41) García-Landeros, S. A.; Cervantes-Díaz, J. M.; Gutiérrez-Becerra, A.; Pelayo-Vázquez, J. B.; Landazuri-Gomez, G.; Herrera-Ordonez, J.; Pérez-García, M. G. Oil-in-eutectic mixture HIPEs co-stabilized with surfactant and nanohydroxyapatite: ring-opening polymerization for nanocomposite scaffold synthesis. *Chem. Commun.* **2019**, *55*, 12292−12295.
(42) Carranza, A.; Romero-Perez, D.; Almanza-Reyes, H.; Bogdanchikova, N.; Juarez-Moreno, K.; Pojman, J. A.; Mota-Morales, J. D. Nonaqueous Synthesis of Macroporous Nanocomposites Using High Internal Phase Emulsion Stabilized by Nanohydroxyapatite. *Adv. Mater. Interfaces* **2017**, *4*, 1700094.
(43) Bejarano, J.; Benavente, R.; Pérez, E.; Wilhelm, M.; Quijada, R.; Palza, H. Effect of Polymer Structure and Incorporation of Nanoparticles on the Behavior of Syndiotactic Polypropylenes. *Macromol. Chem. Phys.* **2013**, *214*, 2567−2578.
(44) Flores, J. M. B.; García, M. G. P.; Contreras, G. G.; Mendoza, A. C.; Arellano, V. H. R. Polydimethylsiloxane nanocomposite macroporous films prepared via Pickering high internal phase emulsions as effective dielectrics for enhancing the performance of triboelectric nanogenerators. *RSC Adv.* **2021**, *11*, 416−424.
(45) Zhang, S.; Fan, X.; Zhang, F.; Zhu, Y.; Chen, J. Synthesis of Emulsion-Templated Magnetic Porous Hydrogel Beads and Their Application for Catalyst of Fenton Reaction. *Langmuir* **2018**, *34*, 3669−3677.
(46) Arora, R.; Balasubramanian, K. Hierarchically porous PVDF/nano-SiC foam for distant oil-spill cleanups. *RSC Adv.* **2014**, *4*, 53761−53767.
(47) Ghosh, G.; Vílchez, A.; Esquena, J.; Solans, C.; Rodríguez-Abreu, C. Preparation of Porous Magnetic Nanocomposite Materials Using Highly Concentrated Emulsions as Templates. In *Trends in Colloid and Interface Science XXIV*; Springer Berlin Heidelberg: Berlin, Heidelberg, 2011, 161−164.
(48) Li, T.; Liu, H.; Zeng, L.; Yang, S.; Li, Z.; Zhang, J.; Zhou, X. Macroporous magnetic poly(styrene−divinylbenzene) nanocomposites prepared via magnetite nanoparticles-stabilized high internal phase emulsions. *J. Mater. Chem.* **2011**, *21*, 12865.
(49) Zhang, T.; Zhao, Y.; Silverstein, M. S. Cellulose-based, highly porous polyurethanes templated within non-aqueous high internal phase emulsions. *Cellulose* **2020**, *27*, 4007−4018.
(50) Zhou, J.; Wang, L.; Qiao, X.; Binks, B. P.; Sun, K. Pickering emulsions stabilized by surface-modified Fe3O4 nanoparticles. *J. Colloid Interface Sci.* **2012**, *367*, 213−224.
(51) Low, L.; Tey, B.; Ong, B.; Chan, E.; Tang, S. Palm olein-in-water Pickering emulsion stabilized by Fe3O4-cellulose nanocrystal nanocomposites and their responses to pH. *Carbohydr. Polym.* **2017**, *155*, 391−399.
(52) Udoetok, I. A.; Wilson, L. D.; Headley, J. V. Stabilization of Pickering Emulsions by Iron oxide Nano-particles. *Adv. Mater. Sci.* **2016**, *1*, 24−33.
(53) Lin, Z.; Zhang, Z.; Li, Y.; Deng, Y. Magnetic nano-Fe3O4 stabilized Pickering emulsion liquid membrane for selective extraction and separation. *Chem. Eng. J.* **2016**, *288*, 305−311.
(54) Lan, Q.; Liu, C.; Yang, F.; Liu, S.; Xu, J.; Sun, D. Synthesis of bilayer oleic acid-coated Fe3O4 nanoparticles and their application in pH-responsive Pickering emulsions. *J. Colloid Interface Sci.* **2007**, *310*, 260−269.
(55) Menner, A.; Verdejo, R.; Shaffer, M.; Bismarck, A. Particle-stabilized surfactant-free medium internal phase emulsions as templates for porous nanocomposite materials: Poly-pickering-foams. *Langmuir* **2007**, *23*, 2398−2403.
(56) Ikem, V. O.; Menner, A.; Bismarck, A. High Internal Phase Emulsions Stabilized Solely by Functionalized Silica Particles. *Angew. Chem., Int. Ed.* **2008**, *48*, 632−632.
(57) Ye, Y.; Jin, M.; Wan, D. One-pot synthesis of porous monolith-supported gold nanoparticles as an effective recyclable catalyst. *J. Mater. Chem. A* **2015**, *3*, 13519−13525.
(58) Vallejo-Macías, M. T.; Recio-Colmenares, C. L.; Pelayo-Vázquez, J. B.; Gómez-Salazar, S.; Carvajal-Ramos, F.; Soltero-Martínez, J. F.; Vázquez-Lepe, M.; Mota-Morales, J. D.; Pérez-García, M. G. Macroporous Polyacrylamide γ-Fe2O3Nanoparticle Composites as Methylene Blue Dye Adsorbents. *ACS Appl. Nano Mater.* **2020**, *3*, 5794−5806.
(59) Huerta-Marcial, S. T.; Mota-Morales, J. D. Tailoring the morphology of poly(high internal phase emulsions) synthesized by using deep eutectic solvents. *E-Polymers* **2020**, *20*, 185−193.
(60) Smith, E. L.; Abbott, A. P.; Ryder, K. S. Deep Eutectic Solvents (DESs) and Their Applications. *Chem. Rev.* **2014**, *114*, 11060−11082.
(61) Carranza, A.; Pojman, J. A.; Mota-Morales, J. D. Deep-eutectic solvents as a support in the nonaqueous synthesis of macroporous poly(HIPEs). *RSC Adv.* **2014**, *40*, 41584−41587.
(62) D'Agostino, C.; Harris, R. C.; Abbott, A. P.; Gladdena, L. F.; Mantle, M. D. Molecular motion and ion diffusion in choline chloride based deep eutectic solvents studied by 1 H pulsed field gradient NMR spectroscopy. *Phys. Chem. Chem. Phys.* **2011**, *13*, 21383−21391.
(63) Yadav, A.; Pandey, S. Densities and Viscosities of (Choline Chloride + Urea) Deep Eutectic Solvent and Its Aqueous Mixtures in the Temperature Range 293. 15 K to 363.15 K. *J. Chem. Eng. Data* **2014**, *59*, 2221−2229.
(64) Pulko, I.; Krajnc, P. High Internal Phase Emulsion Templating - A Path To Hierarchically Porous Functional Polymers. *Macromol. Rapid Commun.* **2012**, *33*, 1731−1746.
(65) Zou, S.; Yang, Y.; Liu, H.; Wang, C. Synergistic stabilization and tunable structures of Pickering high internal phase emulsions by nanoparticles and surfactants. *Colloids Surf., A* **2013**, *436*, 1−9.
(66) Yuan, Q.; Williams, R. A. CO-stabilisation mechanisms of nanoparticles and surfactants in Pickering Emulsions produced by membrane emulsification. *J. Membr. Sci.* **2016**, *497*, 221−228.
(67) Binks, B. P.; Rodrigues, J. A.; Frith, W. J. Synergistic Interaction in Emulsions Stabilized by a Mixture of Silica Nanoparticles and Cationic Surfactant. *Langmuir* **2007**, *23*, 3626−3636.
(68) Binks, B. P.; Desforges, A.; Duff, D. G. Synergistic Stabilization of Emulsions by a Mixture of Surface-Active Nanoparticles and Surfactant. *Langmuir* **2007**, *23*, 1098−1106.
(69) Zhu, Y.; Wang, W.; Yu, H.; Wang, A. Preparation of porous adsorbent via Pickering emulsion template for water treatment: A review. *J. Environ. Sci.* **2020**, *88*, 217−236.
(70) Anderson, J. L.; Pino, V.; Hagberg, E. C.; Sheares, V. V.; Armstrong, D. W. Surfactant solvation effects and micelle formation in ionic liquids. *Chem. Commun.* **2003**, *3*, 2444−2445.
(71) Inoue, T.; Misono, T. Cloud point phenomena for POE-type nonionic surfactants in a model room temperature ionic liquid. *J. Colloid Interface Sci.* **2008**, *326*, 483−489.
(72) Kunieda, H.; Yano, N.; Solans, C. The stability of gel-emulsions in a water/nonionic surfactant/oil system. *Colloids Surf.* **1989**, *36*, 313−322.
(73) Mandal, M.; Kundu, S.; Ghosh, S. K.; Panigrahi, S.; Sau, T. K.; Yusuf, S. M.; Pal, T. Magnetite nanoparticles with tunable gold or silver shell. *J. Colloid Interface Sci.* **2005**, *286*, 187−194.

https://doi.org/10.1021/acsomega.2c01836
ACS Omega 2022, 7, 21763−21774

(74) Rajan, G. S.; Stromeyer, S. L.; Mauritz, K. A.; Miao, G.; Mani, P.; Shamsuzzoha, M.; Nikles, D. E.; Gupta, A. Superparamagnetic nanocomposites based on poly(styrene-b-ethylene/butylene- b-styrene)/cobalt ferrite compositions. *J. Magn. Magn. Mater.* **2006**, *299*, 211−218.
(75) Yang, S.; Liu, H.; Zhang, Z. Fabrication of Novel Multihollow Superparamagnetic Magnetite/Polystyrene Nanocomposite Microspheres via Water-in-Oil-in-Water Double Emulsions. *Langmuir* **2008**, *24*, 10395−10401.
(76) Zhang, N.; Zhong, S.; Zhou, X.; Jiang, W.; Wang, T.; Fu, J. Superhydrophobic P (St-DVB) foam prepared by the high internal phase emulsion technique for oil spill recovery. *Chem. Eng. J.* **2016**, *298*, 117−124.

https://doi.org/10.1021/acsomega.2c01836
ACS Omega 2022, 7, 21763−21774